

Passive AC network supplying the integration of CCC-HVDC and VSC-HVDC systems

Ali BIDADFAR¹, Mehrdad ABEDI^{1,*}, Mehdi KARRARI¹,
Gevork Babamalek GHAREHPETIAN¹, Sanaz Namayan TAVANA²

¹Electrical Engineering Department, Amirkabir University of Technology, Tehran, Iran

²Electrical Engineering Department, Shahabdanesh Institute, Qom, Iran

Received: 15.07.2012 • Accepted: 03.12.2012 • Published Online: 17.01.2014 • Printed: 14.02.2014

Abstract: The integration of a capacitor-commutated converter (CCC) high-voltage direct current (HVDC) (CCC-HVDC) and voltage source converter (VSC) HVDC (VSC-HVDC) is proposed in this paper to supply entirely passive AC networks. The key point of this integration is the flat characteristic of the DC voltage of the CCC-HVDC, which provides the condition for the VSC to connect to the CCC DC link via a current regulator. The advantages of the proposed combined infeeding system are the requirement of only one DC line, and better dynamic responses. The structure of the proposed infeeding system, as well as its control system, is studied. Simulation results are provided to validate the effectiveness of the proposed system and its control strategy. Two other schemes for infeeding AC passive networks are studied to demonstrate the advantages of the proposed system.

Key words: Capacitor-commutated converter, HVDC, voltage source converter, passive network

1. Introduction

To supply entirely passive AC networks, the use of high-voltage direct current (HVDC) power transmission systems is a subject of great interest. Since the AC passive network is a weak system and HVDC converters require relative strength to work properly, some methods must be used to provide the relative strength to passive networks. Aside from AC voltage support, these methods provide the reactive power of the HVDC converters. These methods can be referred to in the literature [1–6]. The traditional devices to meet the requirements of HVDC converters for connecting to passive networks used to be synchronous condensers [1]. Static compensators are used to provide the reactive power for line-commutated converter (LCC)-HVDCs [2,3]. In [4], a static VAR compensator (STATCOM) was used along with a HVDC converter to supply an entirely passive AC system. In [5], the simultaneous application of a STATCOM and capacitor-commutated converter (CCC)-HVDC was proposed to supply a passive AC network. In [6], a double-infeed system consisting of a LCC-HVDC and voltage source converter (VSC)-HVDC was used to supply a passive AC network.

A VSC-HVDC can supply passive AC networks without local generation [7–11]. A VSC-HVDC uses the pulse-width modulation (PWM) technique to generate an AC voltage with the desired amplitude and phase angle [12]. However, when the VSC-HVDC is connected to a weak power system, some problems can arise in its control process [13].

*Correspondence: abedi2@aut.ac.ir

This paper proposes the combination of a CCC-HVDC and VSC-HVDC to supply a passive AC network. The schematic diagram of this combination is shown in Figure 1. This structure benefits from 2 advantages: it has only 1 DC line, and consequently, 1 DC supply; moreover, the VSC can participate in an active power transfer, which can be used for stability improvement in transient conditions.

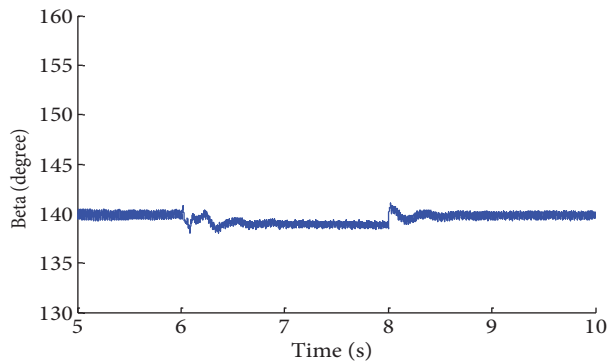


Figure 1. Combination of the CCC-HVDC and VSC-HVDC.

To study the proposed structure, this paper is arranged as follows. In Section 2, the proposed infeeding system is detailed. In Section 3, the principal of the integration of the CCC and VSC is outlined. In Section 4, the control systems are proposed, and finally, in Section 5, the simulation results are provided.

2. Proposed infeeding system

The structure of the proposed infeeding system for an entirely passive AC network is demonstrated in Figure 1. The VSC generates balanced 3-phase AC voltages and supplies the determined amount of active power, as well as the required reactive power of CCC. These functions are done by the VSC in steady-state, while the CCC is supplying a main value of the network active power. In transient conditions, the VSC manipulates the active power between the DC line and the AC network to damp the oscillations quickly, and keeps the AC voltage almost constant. The active power manipulation is carried out through a current regulator, which is a gate turn-off (GTO) thyristor series with a small inductor. The current regulator is the unidirectional path, which sends the energy from the receiving end of the DC line to the DC bus of the VSC.

In black-start time, the current regulator establishes the DC voltage of the VSC. The VSC, in turn, generates the 3-phase voltages with the desired amplitude and frequency, while switch K2 is closed and switches K1 and K3 are open (Figure 1). In the second step, switch K1 is closed and the CCC gets ready to supply the power. At last, switch K3 supplies the AC voltage to the network.

3. Principles of proposed integration

The power transfer principal of the LCC is different from that of the VSC. In the LCC, the power transition is adjusted by changing the DC voltage level, while the DC current is kept almost constant. However, in the VSC, the transmitting power is adjusted by the DC current, while its DC voltage is kept almost constant. Consequently, the DC terminals of both converters are inherently different and their direct connection to each other is basically impossible.

When the LCC is connected to a weak AC system, it suffers from valve commutation failures. This drawback is generally compensated for by a commutation capacitor application in series with the valves, and

subsequently, the CCC is developed [14,15]. These capacitors offer additional voltages for the valves, allowing the use of smaller firing angles and extinction angles in the rectifier and inverter, respectively.

One of the main advantages of the CCC over the LCC is the flatness of its DC voltage-current characteristic, which was presented in [16–18], and is illustrated in Figure 2. The flatness of the DC voltage of the CCC is the key point to propose the combination of a CCC and VSC. In fact, the DC bus of the VSC is connected to the point between the DC line and the smoothing reactor of the CCC. The connection between the 2 converters is done via a GTO switch series with a small inductor, as shown in Figure 3.

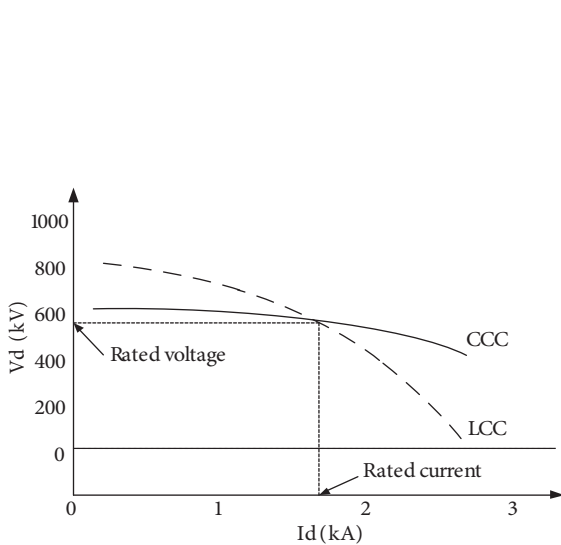


Figure 2. DC current-voltage characteristics of the CCC and LCC [19].

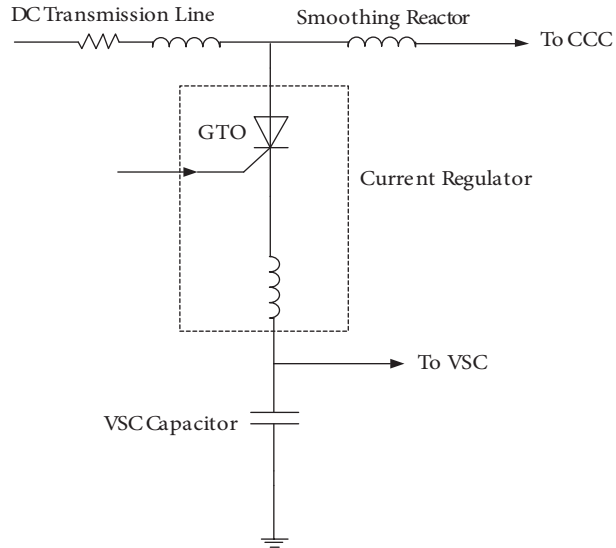


Figure 3. Current regulator.

The inductor in the current regulator avoids the sudden inrush current when the GTO starts conducting at the instant when there exist 2 different voltage levels at both sides. However, this inductance is not too large to cause an unbearable overvoltage across the VSC capacitor.

Connecting the current regulator to the point where the DC line and smoothing reactor are tied, the current flowing toward the VSC will not significantly disturb the CCC DC current. Thus, the normal operation of the CCC will not be affected by the existence of the current regulator.

4. Control system

The main task of the control system is to provide an almost stiff control to both converters, so that an AC voltage with the desired amplitude and frequency is established on a passive network.

It is assumed that the rectifier is operating in constant DC voltage mode so that the inverter can control the network active power. In this paper, the rectifier is represented only by a constant DC voltage. In steady-state operation, the largest percentage of the network active power is delivered by the CCC, and the network AC voltage amplitude, as well as its frequency, is controlled by the VSC. However, in transients, the VSC participates more in the active power transfer so that fast damping of the oscillations occurs.

4.1. VSC control

The VSC is composed of a 3-phase PWM converter, which generates the voltage vector v in its output, and a transformer, which connects the converter to the filter bus with the voltage vector u_f . The converter is controlled by the vector current control, which uses the direct and quadrature (DQ) decoupling technique [19–21]. The basic principle of this control strategy is to control the active power and the reactive power independently through an innercurrent control loop. A simple implementation of a current controller is achieved by the proportional-type control as follows:

$$v_{ref}^c = \alpha_c L_c (i_{ref} - i_c^c) + j\omega L_c i_c^c + H_{LP}(s) u_f^c, \quad (1)$$

where α_c is the desired closed-loop bandwidth of the innercurrent controller, i_{ref} is the converter current reference, v_{ref}^c is the voltage reference of the VSC, and ω is the network angular frequency. The superscript c denotes the converter DQ frame. The term $j\omega L_c i_c^c$ is used to remove the so-called cross-coupling [22]. The function $H_{LP}(s)$ is a low-pass filter to improve the disturbance rejection capability of the current controller. $H_{LP}(s)$ has the following expression:

$$H_{LP}(s) = \frac{\alpha_f}{s + \alpha_f}, \quad (2)$$

where α_f is typically chosen with a bandwidth (40–100 rad/s) [23]. The direct and quadrature components of i_{ref} are obtained from the active power controller and alternating-voltage controller, respectively. These 2 controllers are simply the proportional-integral (PI)-controller types, which are presented by Eqs. (3), and (4).

$$i_{ref}^d = \left(K_p^P + \frac{K_i^P}{s} \right) [P_{ref}^{vsc} - P^{vsc}] \quad (3)$$

$$i_{ref}^q = \left(K_p^U + \frac{K_i^U}{s} \right) [U_{ref} - U_f] \quad (4)$$

In the vector current control, the DQ components of the converter current always follow the corresponding current references. Consequently, by limiting the modulus of the current references, the valve current of the converter is limited in the fault condition. The main circuit and control block diagram of the VSC are shown in Figure 4, in which L_c is the leakage inductance of the connecting transformer. The output of the control block diagram is the 3-phase AC reference signal, which is fed to the PWM section to generate the firing pulses for the VSC switches.

4.2. CCC control

The CCC control is based on delivering the largest percentage of the network active power. However, with the proposed structure of the infeeding system, the VSC can participate in the active power transmission as well. The CCC control block diagram is presented in Figure 5, where P_{load} is the network total active power, P_{vsc} is the VSC active power, P_{ref}^{ccc} is the reference value of the CCC active power, and P_{loss}^{ccc} is the power losses through the CCC and smoothing reactor. The V_{dc}^{ccc} is the receiving-end voltage of the DC line and I_{ref}^{ccc} is the reference value of the DC current flowing through the CCC. The I_{ref}^{ccc} is compared with its corresponding measured value, I_{ccc} , and the resultant is given to the PI-controller to generate the CCC valve firing pulses. On the other hand, the extinction angle, γ , is measured to ensure that the firing angle is not too large to cause a commutation failure in the converter.

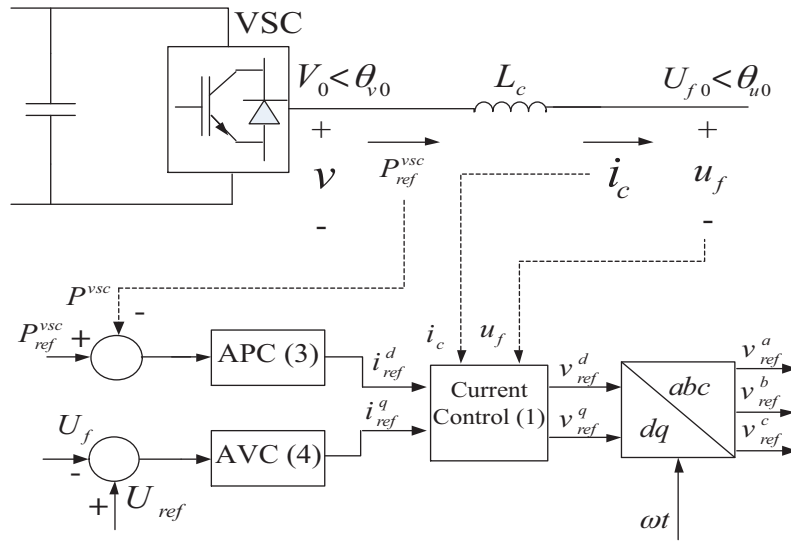


Figure 4. Main circuit and control block diagram of the VSC using current vector control.

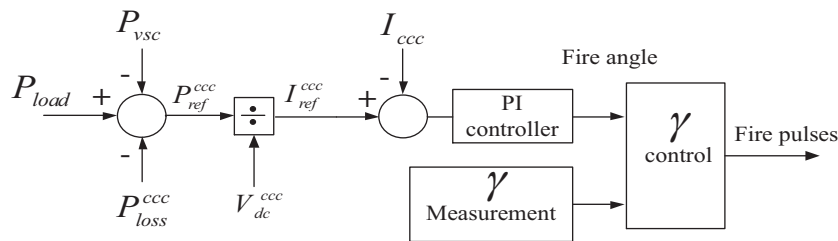


Figure 5. Control block-diagram of the CCC.

4.3. VSC DC-voltage control

As mentioned earlier, the VSC DC voltage is energized by the DC line voltage through the current regulator. When the measured value of the VSC DC voltage is lower than its reference value, the current will be conducted from the DC line to the VSC DC capacitor. On the other hand, a predetermined amount of VSC active power, P_{ref}^{vsc} , will not allow the VSC DC capacitor to be overcharged.

5. Simulation studies

To validate the proposed structure of the passive network infeeding system, simulation studies are carried out by PSCAD/EMTDC for different conditions. In the simulations, the schematic diagram shown in Figure 1 is used for the infeeding system and the control block diagrams shown in Figures 4 and 5 are used for the VSC and CCC control, respectively. The passive network is a 230-kV 50-Hz system with a 410-MW passive load and 100-MW motor load. As mentioned earlier, the DC line voltage is controlled by a rectifier station, which is not considered in the studies. The DC line is modeled with a 0.2-Ohm resistance in series with an inductance of 0.1 H. The CCC series capacitor is of a 0.3-mF capacitance and the VSC capacitor is 0.2 mF. The smoothing reactor of the CCC has a 0.5-H inductance and that of the current regulator is 0.0001 H. The CCC transformer has a 1000-MVA power capacity with a 0.15-pu leakage inductance, and the VSC transformer has 500 MVA of power and a 0.1-pu leakage inductance. Both transformers possess 0.04-pu copper losses. The capacitive filter in the AC network has 35 MVAR of reactive power. K_p^P and K_i^P are equal to 20 and 100 rad/s, respectively.

K_p^U and K_i^U are set to 10 and 80 rad/s. In addition, the CCC PI-controller gains are 10 and 100 rad/s. Three different simulations are carried out as follows.

5.1. Network load changing

In this simulation, 2 scenarios are considered. In the first one, at 6.0 s, a 45-MW motor load is added to the network; and in the second one, 50 MW of active power is shifted from the CCC to the VSC at 8.0 s. Figures 6–10 show the responses to these changes. As shown in Figure 6, after the motor load connection, the VSC takes that incoming load instantly, because the VSC is faster than the CCC. In addition, when the 50 MW of power is transferred from the CCC to the VSC, there are no significant oscillations in the load active power. This is because the amplitude and frequency of the AC voltage are not considerably affected. Figure 7 proves the stiffness of the voltage amplitude. As shown in Figure 8, the VSC DC voltage is adjusted to 190 kV. However, the new added load is not supposed to be supplied by the VSC; thus it is transferred from the VSC to the CCC by adjusting the CCC firing angle shown in Figure 9.

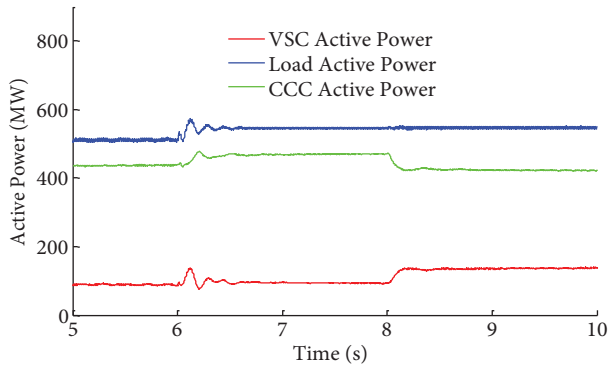


Figure 6. Active powers of load, CCC, and VSC.

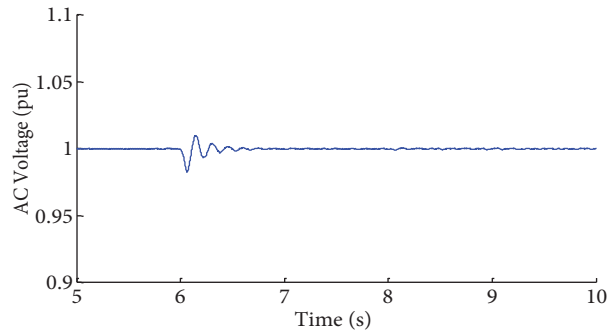


Figure 7. The network AC voltage.

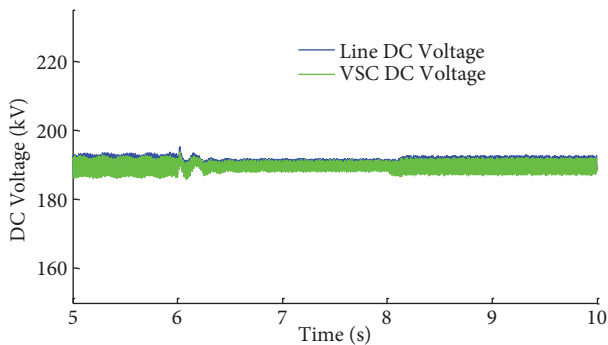


Figure 8. Voltages of the DC line and VSC DC bus.

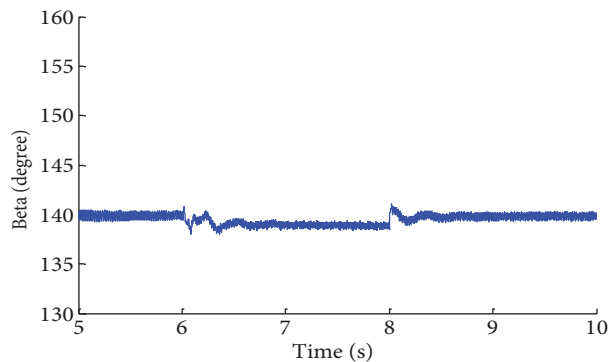


Figure 9. CCC firing angle.

The induction motor speed, the one connected earlier, is shown in Figure 10, which demonstrates that the entrance of the new load and power shifting between the converters has no substantial effect on the induction motor speed.

5.2. Reduction of the DC voltage

Another scenario is considered as the reduction of the DC line voltage. In this case, the supplying DC voltage drops to 20% lower than its nominal value, as shown in Figures 11–13. When the voltage reduction occurs,

the deviation of the load active power is not substantial in comparison with those of the CCC and VSC active powers, as shown in Figure 12. The active power of the CCC is reduced because of the DC voltage fall; on the other hand, the active power of the VSC is increased immediately to compensate for the CCC power reduction.

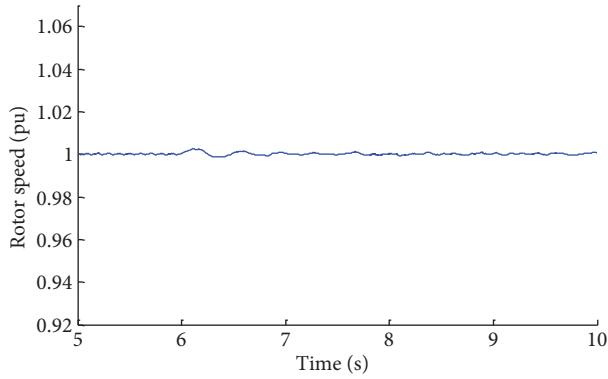


Figure 10. Rotor speed of the induction motor (pu).

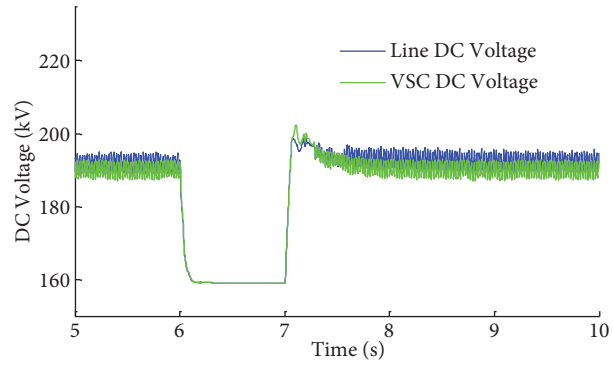


Figure 11. Voltages of the DC line and VSC DC bus when the DC line voltage drops by 20%.

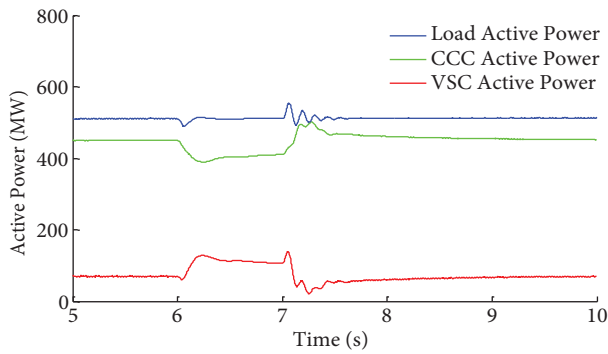


Figure 12. Active powers of the load, CCC, and VSC when the DC line voltage drops by 20%.

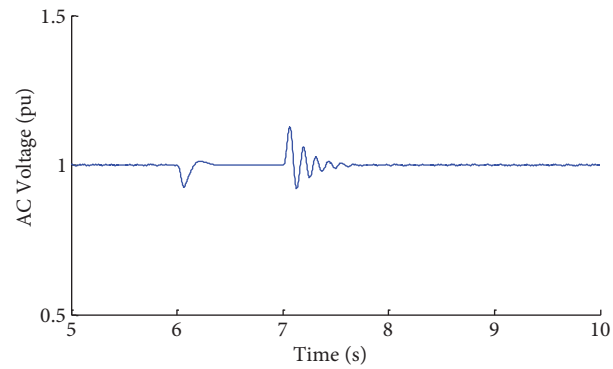


Figure 13. AC voltage of the network when the DC line voltage drops by 20%.

To make more comparisons, 2 other schemes of infeeding systems are studied herein. As mentioned previously, in [6], an infeeding system composed of a LCC-HVDC and VSC-HVDC with 2 separate DC lines was used, known as a double-infeed system. Here, for this system, it is used to make a comparison with the proposed structure. However, in the double-infeed system, a CCC is used instead of a LCC in this paper. The same scenario, a CCC DC voltage reduction by 20%, is considered when a CCC and VSC with 2 separate DC lines comprise the infeeding system. For this system, the active power curves of the CCC, VSC, and load are shown in Figure 14.

The curves in Figures 12 and 14 are almost the same; however, the power variations in Figure 14 are lower than those in Figure 12. This is because when 2 separate DC lines are used, the VSC DC voltage is not directly subjected to the sudden reduction of the CCC DC voltage. Nevertheless, the scheme proposed in this paper benefits from having only 1 DC line.

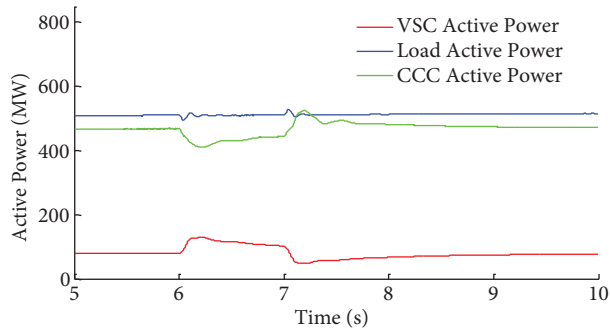


Figure 14. Active powers of the load, CCC, and VSC under DC voltage reduction when 2 separate DC lines are used.

Another simulation is carried out for an infeeding system made of a CCC-HVDC and STATCOM, which was introduced in [5]. In that system, the CCC operates with constant power and the STATCOM is controlled by the strategy given in [5]. The STATCOM, with a 0.2-mF capacitance in its DC bus, cannot support the network AC voltage; therefore, the infeeding system fails, as shown in Figure 15. The STATCOM capacitor is increased to 2.0 mF in this study to improve the infeeding system stability. Moreover, it is clear from Figure 16 that the load and CCC power are reduced during the fault. This is because the CCC is working with its maximum firing angle, and consequently, with its maximum current, so that the power reduction cannot be compensated more.

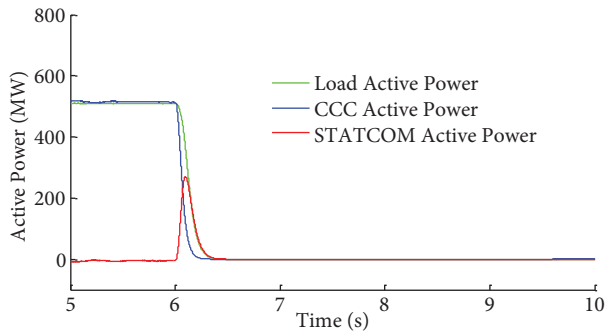


Figure 15. Active powers of the load, CCC, and STATCOM under DC voltage reduction when the capacitance of the STATCOM DC link is 0.2 mH.

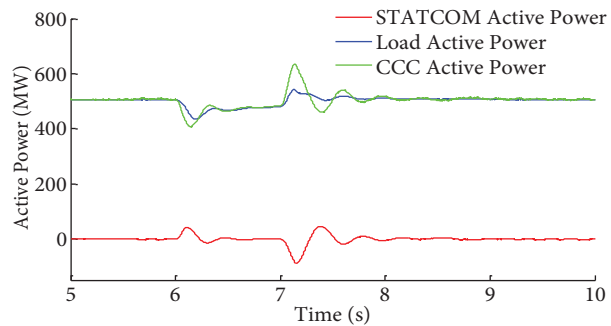


Figure 16. Active powers of the load, CCC, and STATCOM under DC voltage reduction when the capacitance of the STATCOM DC link is 2.0 mH.

5.3. Shot-circuit fault occurrence

A single-phase short circuit occurs in the AC side, where 2 converters are connected to the loads. The fault occurs at 6.0 s and is cleared at 0.7 s, as shown in Figure 17. To compare the proposed infeeding system with the other 2 aforementioned systems under the same fault condition, the results are presented in Figures 18–20. As shown in the curves, there is no major difference between the responses of the proposed system with those of the double-infeed system. Nevertheless, when the CCC and STATCOM are supplying the passive network, the oscillations in the active power are significant.

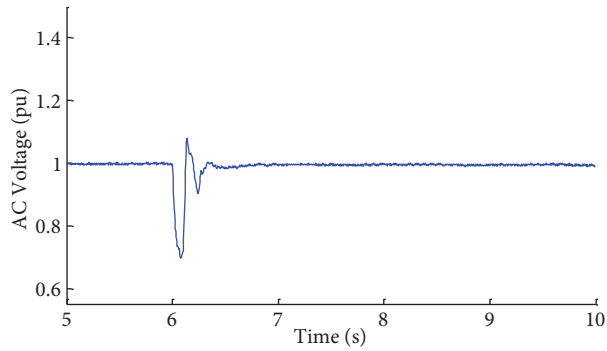


Figure 17. AC Voltage in per-unit under the short circuit fault.

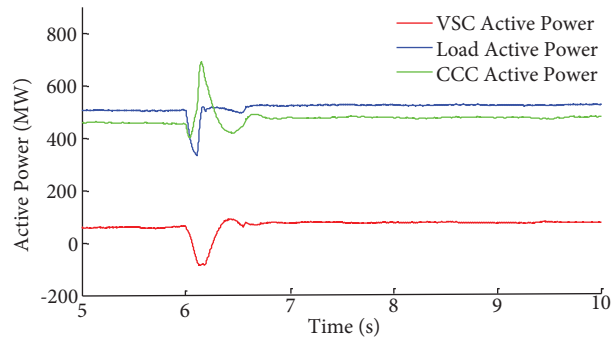


Figure 18. Active powers of the load, CCC, and VSC under the single-phase short-circuit fault when the network is infed by the proposed system (1 DC line is used for both converters).

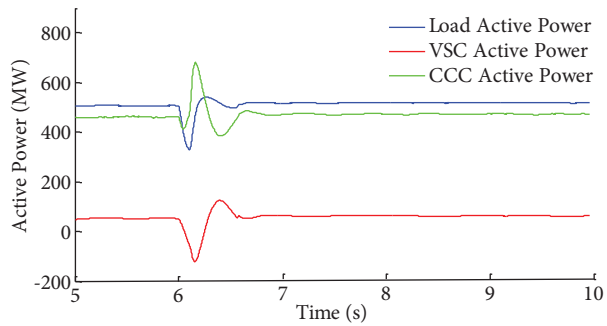


Figure 19. Active powers of the load, CCC, and VSC under the single-phase short-circuit fault when 2 separate DC lines are used for converters.

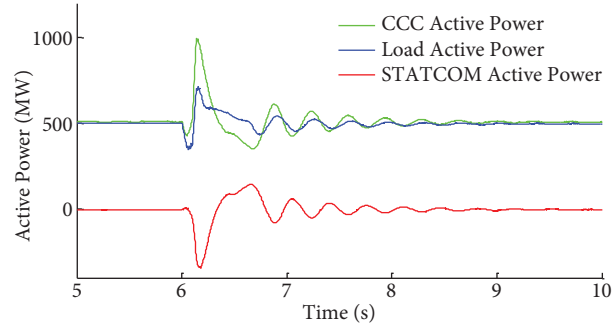


Figure 20. Active powers of the load, CCC, and STATCOM under the single-phase short-circuit fault.

6. Conclusion

In this paper, a new passive network infeeding system composed of a CCC and VSC-HVDC is proposed. It is shown that the VSC can participate in the active power transition and share the infeeding load to the network. Simulation results are presented for different scenarios to confirm the effectiveness of the proposed infeeding system. Moreover, it is shown that the proposed system has almost the same performance as the system composed of a CCC and VSC with 2 separate DC lines; nevertheless, the proposed system benefits from having only 1 DC line. In comparison with the infeeding system made of a CCC and STATCOM, the proposed system reveals more safety and ability of supplying the load power.

References

- [1] C.V. Thio, J.B. Davies, "New synchronous compensators for the nelson river HVDC system-planning requirements and specifications", IEEE Transactions on Power Delivery, Vol. 6, pp. 922–928, 1991.
- [2] Y. Zhuang, R.W. Menzies, O.B. Nayak, H.M. Turanli, "Dynamic performance of a STATCOM at an HVDC inverter feeding a very weak AC system", IEEE Transactions on Power Delivery, Vol. 11, pp. 958–964, 1996.

- [3] O.B. Nayak, A.M. Gole, D.G. Chapman, J.B. Davies, "Dynamic performance of static and synchronous compensators at an HVDC inverter bus in a very weak AC system", *IEEE Transactions on Power Systems*, Vol. 9, pp. 1350–1358, 1994.
- [4] M. DeOliveira, M. Poloujadoff, A. LeDu, P.G. Therond, "Supply of an entirely passive AC system through an HVDC link", *International Journal of Electrical Power & Energy Systems*, Vol. 16, pp. 111–116, 1994.
- [5] B.R. Andersen, L. Xu, "Hybrid HVDC system for power transmission to island networks", *IEEE Transactions on Power Delivery*, Vol. 19, pp. 1884–1890, 2004.
- [6] C. Guo, C. Zhao, "Supply of an entirely passive AC network through a double-infeed HVDC system", *IEEE Transactions on Power Electronics*, Vol. 24, pp. 2835–2541, 2010.
- [7] G. Zhang, Z. Xu, H. Liu, "Supply passive networks with VSC-HVDC", *Proceedings of the IEEE/PES Summer Meeting*, 2001.
- [8] C.K. Sao, P.W. Lehn, "Intentional islanded operation of converter fed microgrids", *Proceedings of the IEEE Power Energy Society General Meeting*, 2006.
- [9] C. Du, M.H. J. Bollen, E. Agneholm, and A. Sannino, "A new control strategy of a VSC-HVDC system for high-quality supply of industrial plants", *IEEE Transactions on Power Delivery*, Vol. 22, pp. 2386–2394, 2007.
- [10] C. Zhao, L. Li, G. Li, C. Guo, "A novel coordinated control strategy for improving the stability of frequency and voltage based on VSC-HVDC", *Proceedings of the 3rd International Conference on Electric Utility Deregulation Restructuring and Power Technologies*, pp. 2202–2206, 2008.
- [11] S. Li, M. Zhou, Z. Liu, J. Zhang, Y. Li, "A study on VSC-HVDC based black start compared with traditional black start", *Proceedings of the International Conference on Sustainable Power Generation Supply*, pp. 1–6, 2009.
- [12] G. Ding, M. Ding, G. Tang, "An innovative hybrid PWM technology for VSC in application of VSC-HVDC transmission system", *Proceedings of the Electric Power Conference*, pp. 1–8, 2008.
- [13] L. Zhang, L. Harnefors, H.P. Nee, "Modeling and control of VSC-HVDC links connected to island systems", *IEEE Transactions on Power Systems*, Vol. 26, pp. 783–789, 2011.
- [14] J. Reeve, J.A. Baron, G.A. Hanley, "A technical assessment of artificial commutation of HVDC converters with series capacitors", *IEEE Transactions on Power Apparatus and Systems*, Vol. PAS-87, pp. 1830–1840, 1968.
- [15] Y. Kazachkov, N.Y. Schenectady, "Fundamentals of a series capacitor commutated HVDC terminal", *IEEE Transactions on Power Delivery*, Vol. 13, pp. 1157–1161, 1998.
- [16] K. Sadek, M. Pereira, D.P. Brandt, A.M. Gole, A. Daneshpooy, "Capacitor commutated converter circuit configurations for DC transmissions", *IEEE Transactions on Power Delivery*, Vol. 13, pp. 1257–1264, 1998.
- [17] M. Meisingset, A.M. Gole, "A comparison of conventional and capacitor commutated converters based on steady-state and dynamic considerations", *Proceedings of the 7th International Conference on AC-DC Power Transmission*, pp. 49–54, 2001.
- [18] F. Yang, Y. Chang, "Study on capacitor commutated converter applied in HVDC projects", *PES General Meeting*, pp. 1–5, 2007.
- [19] M.P. Kazmierkowski, R. Krishnan, F. Blaabjerg, *Control in Power Electronics*, Massachusetts, Academic Press, 2002.
- [20] J.W. Choi, S.K. Sul, "Fast current controller in three-phase AC/DC boost converter using d-q axis crosscoupling", *IEEE Transactions on Power Electronics*, Vol. 13, pp. 179–185, 1998.
- [21] M.P. Kazmierkowski, L. Malesani, "Current control techniques for three-phase voltage-source PWM converters: a survey", *IEEE Transactions on Industrial Electronics*, Vol. 45, pp. 691–703, 1998.
- [22] L. Zhang, "Modeling and control of VSC-HVDC links connected to weak AC systems", *PhD Dissertation*, Royal Institute of Technology, Stockholm, Sweden, 2010.
- [23] L. Harnefors, M. Bongiorno, S. Lundberg, "Input-admittance calculation and shaping for controlled voltage-source converters", *IEEE Transactions on Industrial Electronics*, Vol. 54, pp. 3323–3334, 2007.